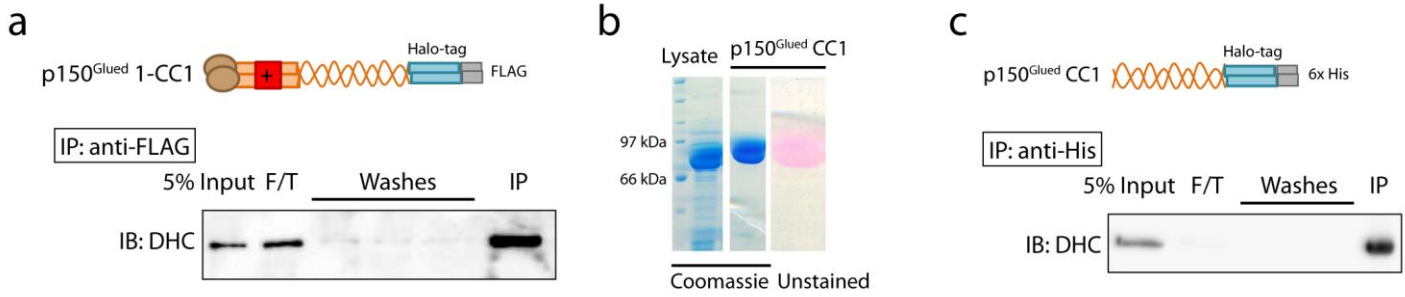


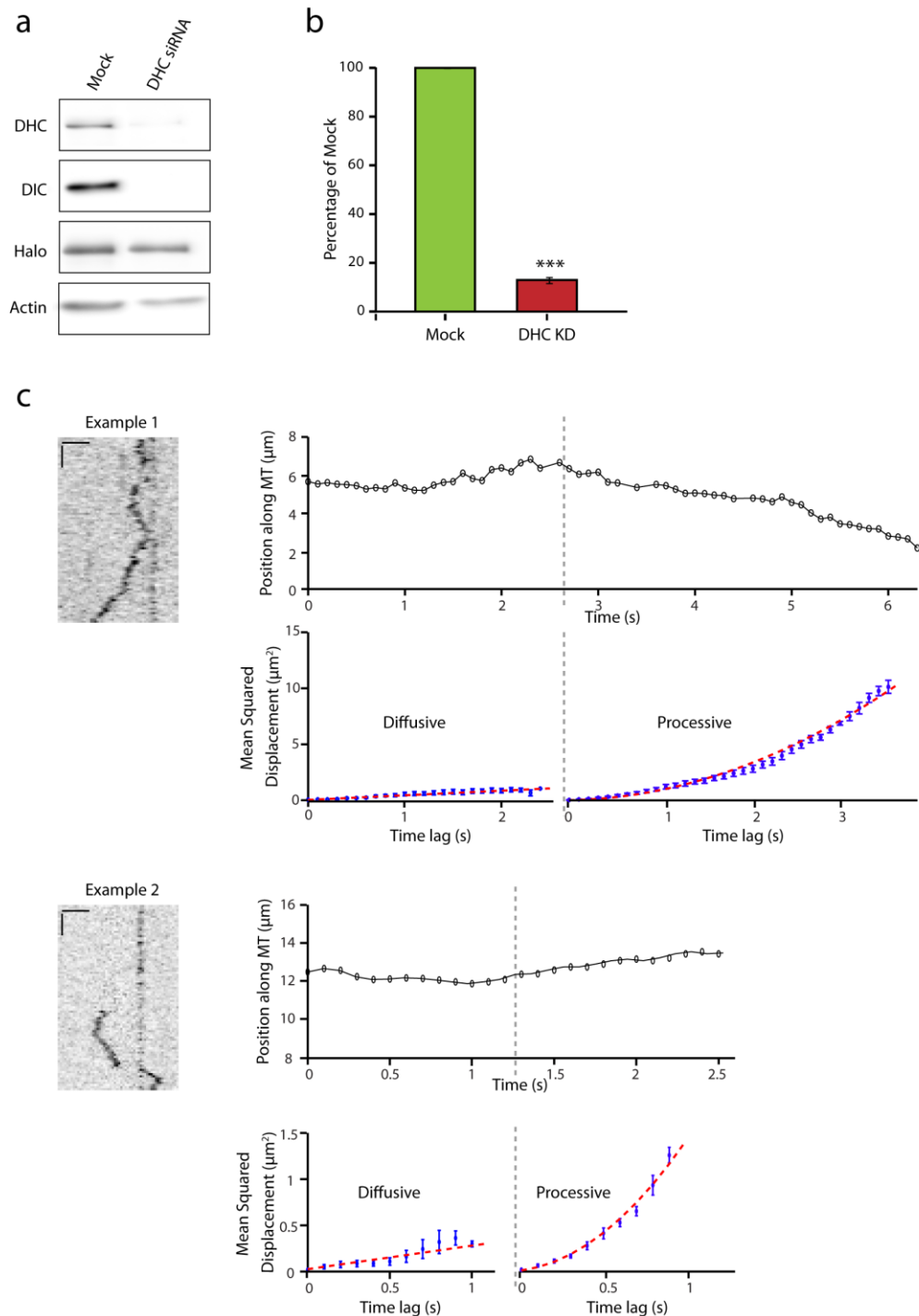
**Supplementary Figure 1. Photobleaching data and simulations to validate GrAND, related to Figure 1.**

(a) A representative time course of photobleaching showing two steps of decay. Grey lines indicate the steps. (b) Frequency distribution of the photobleaching steps for  $n=40$  particles fit with a binomial distribution. (c) To demonstrate that the dynein runs are not terminated by photobleaching, the average time taken for the complete photobleaching of the dynein molecules ( $n=30$ ) with 1 standard deviation is superimposed on a cumulative frequency plot of the track duration of all the dynein particles tracked ( $n=112$ ). 95% of the dynein particles tracked are bound for less than 60 seconds while the average time required to photobleach GFP in our system was 72 seconds. (d) Leading edges of two microtubules marked in a gliding assay with purified dynein. Scale bar, 5  $\mu\text{m}$ . (e) 50 simulated tracks shown for 3 different conditions – purely diffusive motion ( $P_p=0$ ,  $P_d=1$ ), a mix of diffusion and processive motion ( $P_p=0.5$ ,  $P_d=0.5$ ) and fully processive motion ( $P_p=1$ ,  $P_d=0$ ).

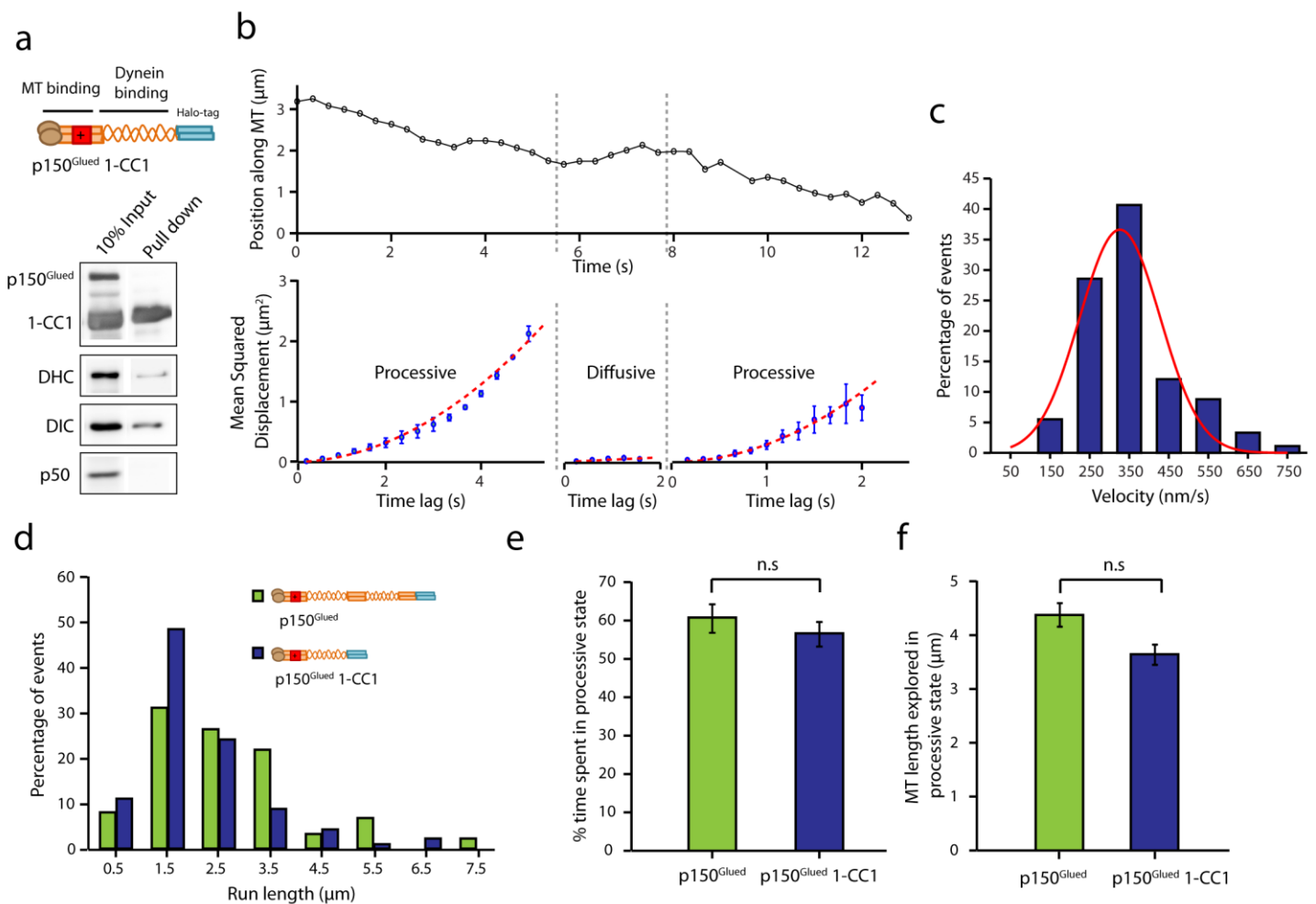


**Supplementary Figure 2. Binding experiments of the recombinant purified proteins, related to Figure 2.**

(a) Recombinant p150<sup>Glued</sup> 1-CC1 binds to purified bovine dynein as shown by the immunoblot. (b) Coomassie stained gel showing the lysate and the protein p150<sup>Glued</sup> CC1 after the final purification step. The unstained gel shows the labeling of the protein with TMR. (c) Recombinant p150<sup>Glued</sup> CC1 binds to purified bovine dynein as shown by the immunoblot.

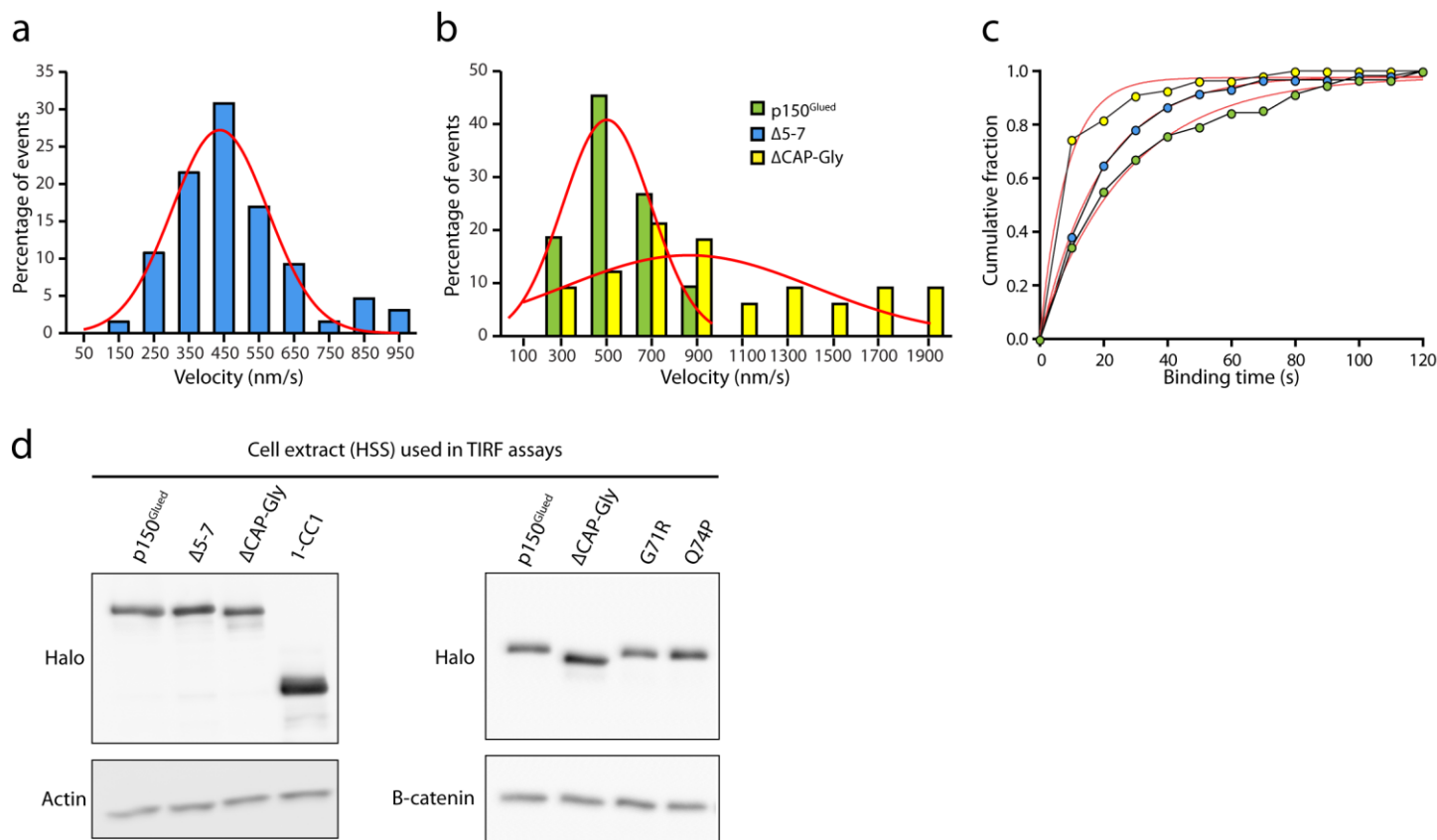


**Supplementary Figure 3. The motility of p150<sup>Glued</sup> in cell extracts is dynein dependent, related to Figure 4.** (a) Representative immunoblot of cell extracts from COS7 cells treated with Mock or DHC siRNA followed by transient transfection of p150<sup>Glued</sup>-Halo. (b) Quantification of the knock down with actin as the loading control. Mean  $\pm$  SEM, n=3 independent experiments, \*\*\*p<0.001, Student's t test. (c) Representative kymographs and the corresponding MSD analysis of p150<sup>Glued</sup>-Halo in motility assays with cell extract generated from movies acquired at 10 frames per second. Horizontal bar, 2  $\mu\text{m}$ . Vertical bar, 1 s. Error bars indicate SEM. The kymographs are contrast inverted.



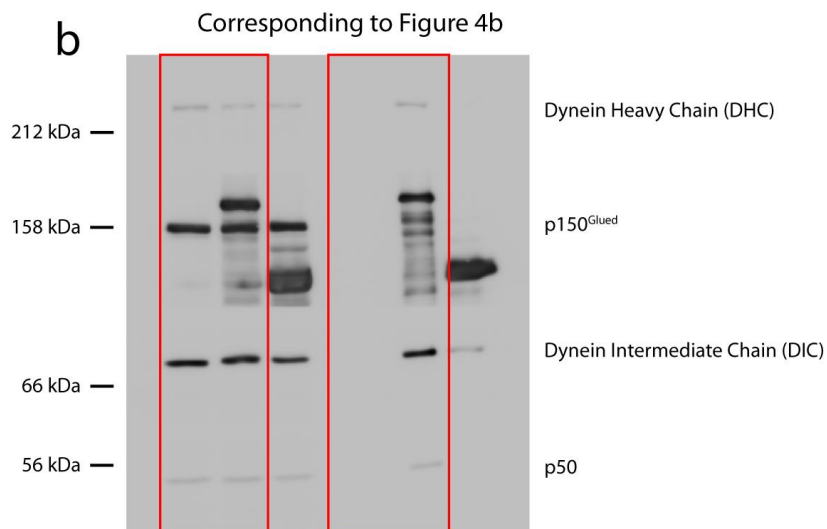
**Supplementary Figure 4. p150<sup>Glued</sup> 1-CC1 shows motility characteristics similar to full-length p150<sup>Glued</sup>.**

(a) COS7 extracts expressing p150<sup>Glued</sup> 1-CC1-Halo were precipitated by the HaloLink resin. Immunoblot analysis shows the truncation does not affect the binding to dynein but inhibits incorporation into the dynactin complex (shown by p50). (b) An example trajectory of this construct and its MSD analysis. Error bars indicate SEM. The particle switches from processive to diffusive state and switches back to processive again. (c and d) Velocity and run length distributions show no significant differences (Mann-Whitney U-test) between the p150<sup>Glued</sup> 1-CC1 and p150<sup>Glued</sup>. (n=91 and 87 processive segments respectively obtained from 60 tracked particles each, 3 independent experiments). (e) A slight decrease was observed in the percent time spent in processive state for p150<sup>Glued</sup> 1-CC1 when compared to the full-length. Mean ± SEM, n.s., not significant, Student's t-test. (f) A similar trend was observed in the microtubule distance explored by the two constructs. Mean ± SEM, n.s., not significant, Student's t-test.



**Supplementary Figure 5. Analysis of the  $\Delta 5-7$  and  $\Delta \text{CAP-Gly}$  in comparison the full-length  $\text{p150}^{\text{Glu}}$ , related to Figure 5.**

(a) Velocity distribution of the all the  $\Delta 5-7$  particles tracked ( $n=60$ , 3 independent experiments) (b) Velocity distributions of the  $\Delta \text{CAP-Gly}$  ( $n=40$ , 3 independent experiments) in comparison to  $\text{p150}^{\text{Glu}}$  ( $n=60$ , 3 independent experiments, same data as in Fig. 3e replotted for  $\text{p150}^{\text{Glu}}$ ). (c) Cumulative frequency plots of the binding time of the 3 constructs (same data as shown in Fig. 5d). Data points are fit by a one-phase exponential decay (red) with a decay constant of  $k=0.035 \pm 0.003 \text{ s}^{-1}$  for  $\text{p150}^{\text{Glu}}$ ,  $k=0.049 \pm 0.002 \text{ s}^{-1}$  for  $\Delta 5-7$  and  $k=0.11 \pm 0.021 \text{ s}^{-1}$  for  $\Delta \text{CAP-Gly}$ . This indicates that the the loss of CAP-Gly increases the detachment rate 3-fold. (d) Cell extract samples used for TIRF motility assays blotted for Halo tag and actin/B-catenin as the loading control to show that the expression levels of the constructs are comparable.



**Supplementary Figure 6. Uncropped Western blots**

(a) Full western blot of sucrose gradient purified dynein-dynactin complexes. (b) Full western blot of halo resin pull down of p150<sup>Glued</sup>-Halo from COS7 cells. Boxed lanes are shown in Figure 4b.